

A polarized neutron investigation of the martensitic phase transition in V_3Si : evidence for a band Jahn-Teller mechanism

This article has been downloaded from IOPscience. Please scroll down to see the full text article.

2001 J. Phys.: Condens. Matter 13 1111

(<http://iopscience.iop.org/0953-8984/13/5/324>)

View [the table of contents for this issue](#), or go to the [journal homepage](#) for more

Download details:

IP Address: 171.66.16.226

The article was downloaded on 16/05/2010 at 08:30

Please note that [terms and conditions apply](#).

A polarized neutron investigation of the martensitic phase transition in V_3Si : evidence for a band Jahn–Teller mechanism

P J Brown^{1,2}, K-U Neumann¹ and K R A Ziebeck¹

¹ Department of Physics, Loughborough University, Leics LE11 3TU, UK

² Institut Laue–Langevin, Avenue des Martyrs, Grenoble 38042, France

Received 8 November 2000

Abstract

Polarized neutron diffraction has been used to study the structural phase transition in V_3Si . The redistribution of electrons between the two independent V sites in the low-temperature phase of V_3Si has been determined by comparing the magnetic scattering observed from reflections that are equivalent in the high-temperature cubic phase but inequivalent below the transition. The higher susceptibility observed at the twofold, compared with the fourfold, vanadium sites in the tetragonal phase is consistent with the predictions of a band Jahn–Teller model of the phase transition.

1. Introduction

V_3Si is one of the group of A15 compounds which undergo a transition to a tetragonal variant of the A15 structure at a temperature T_M slightly above the superconducting transition temperature T_c . In the case of high-quality V_3Si single crystals, these transitions occur at 21.3 and 17 K, respectively [1]. The crystallographic details for the two phases are given in table 1, and the tetragonal structure is illustrated in figure 1. X-ray diffraction measurements have shown that the deviation of the axial ratio c/a from unity continues to increase below the martensitic transition temperature T_M and saturates at the superconducting transition temperature T_c , suggesting that the onset of superconductivity inhibits further distortion [2]. The ratio c/a is

Table 1. Crystallographic data for the cubic and tetragonal phases of V_3Si .

	Cubic phase	Tetragonal phase
Space group	$Pm\bar{3}n$	$\bar{4}_2/mmc$
Lattice parameters	$a = 4.753 \text{ \AA}$	$a = 4.715 \text{ \AA}, c = 4.725 \text{ \AA}$
Atomic positions	V $6c, \frac{1}{4}0\frac{1}{2}$	$2e, 00\frac{1}{4}$ $4k, x\frac{1}{2}\frac{1}{2}, x \approx \frac{1}{4}$
	Si $2a, 000$	$2c, 0\frac{1}{2}0$

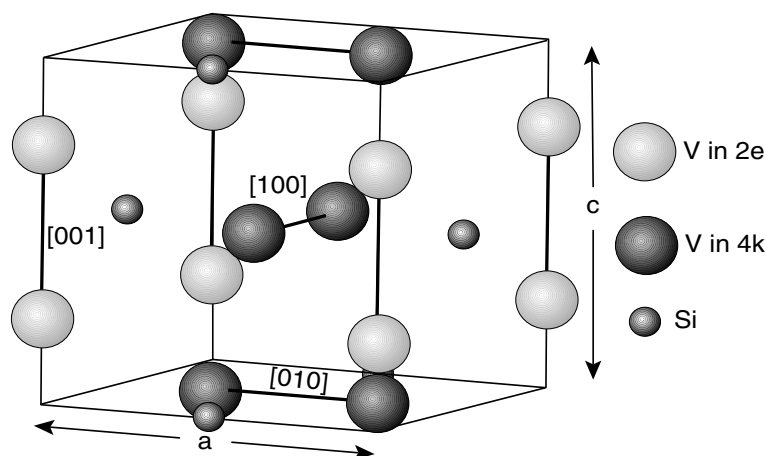


Figure 1. The arrangement of atoms in the tetragonal structure of V_3Si . The V atoms in the 2e sites form chains along the [001] direction whilst those in the 4k sites are in chains along the [100] and [010] directions.

greater than 1 for some compounds of the group, e.g. V_3Si , and less than 1 for others, e.g. Nb_3Sn . The difference from unity of c/a is of order 10^{-3} . More recent x-ray diffraction measurements made below T_M [3] show that the atoms in the V sublattice are displaced relative to one another by an amount proportional to the tetragonal strain, in the same way as in Nb_3Sn [4, 5]. This displacement corresponds to a ‘frozen-in’ optic phonon with Γ_{12} symmetry; this implies that the V atoms on chains along the two a -axes dimerize. The tetragonal distortion is accompanied by a large but incomplete softening of the elastic constant $c' = \frac{1}{2}(c_{11} - c_{12})$. The softening of the corresponding [110] T_1 phonon mode is unusual, because it occurs at wave vectors throughout the zone. The phase transition is almost second order; there is negligible discontinuous change in volume, practically no spontaneous strain [6] and little latent heat [7]. These are just the characteristics of a thermo-elastic martensitic phase transition.

2. Models for the phase transition

The correlation of superconductivity with the structural transition, and related aspects of the electronic instability, has led to considerable theoretical and experimental work on these compounds. As with many martensitic phase transitions, the softening of the phonon mode is incomplete and models based on this mechanism have found only limited application [8]. Susceptibility [9], specific heat [10] and Knight shift [11] measurements all suggest that there is a sharp peak in the density of states within which the Fermi level lies. Accordingly, the models which have been proposed to explain the structural phase transition rely on the proximity of the Fermi surface to such a peak [12–15]. Since the transition metal atoms in the A15 structure form a system of three essentially non-interacting orthogonal linear chains, one dimensionality has been a feature of many models [12]. Those which consider the three-dimensional features of the structure are able to account for many of the structural and electronic properties, but the mechanism underlying the structural phase transition is the same in all of the models [14–16]. Band-structure calculations [14, 15] within the APW approximation predict that two flat bands associated with the Γ_{12} doublet lie within a few mRyd of E_F . As a result, a peak in the density of states is almost coincident with E_F . Near the Γ point these bands consist of $(3z^2 - r^2)$ and

(xz , yz) orbitals with strong hybridization between chains. Extension of the band-structure calculations to the tetragonal phase of Nb₃Sn indicates that the Γ_{12} peak in the density of states splits symmetrically into two sub-peaks, one of which is raised above E_F . This feature of the band structure has led to the suggestion that a band Jahn–Teller mechanism may drive the martensitic phase transition. In a normal Jahn–Teller transition it is the splitting of degenerate energy levels caused by coupling to thermal vibrations which drives the transition. A band Jahn–Teller transition it is driven by a similar splitting of degenerate electron energy bands. The splitting arises because the width of the bands depends on the degree of overlap between wave-functions on neighbouring atoms, and this will change when the structure deforms. The deformation will lead to a structural transition if the change in band structure enables the electrons to redistribute themselves so as to lower the free energy. This mechanism is that invoked in the Labbé–Friedel model [12]. This model assumes that the band structure of the cubic A15 compounds can be represented by three sub-bands of d type inserted into each other and superposed on a wide band of s character. For vanadium compounds the d sub-band is less than half-full, so the Fermi level can be near the bottom of the highest d sub-band, ensuring a high density of states at the Fermi level. In the transition to a tetragonal structure with $c/a > 1$ the width of the band becomes narrower in the [001] direction than in the [100] and [010] directions. The electrons can be accommodated with lower energy in the broader band, giving rise to an effective band splitting.

3. Background to the present experiment

It has been shown recently that it is probably a band Jahn–Teller mechanism which drives the martensitic phase transition in the ferromagnetic shape memory compound Ni₂MnGa [17]. This was achieved by determining the change in the magnetization distribution on traversing the structural phase transition using polarized neutron diffraction and relating this change to the symmetry of the orbitals involved. V₃Si is paramagnetic but the electrons at the Fermi surface of a paramagnetic metal can be magnetized by an applied magnetic field. The distribution of their induced magnetization is to a first approximation proportional to the spatial probability of their wave-function and the magnitude to the susceptibility or local density of states. Hence measurement of the induced magnetization distribution, using the sensitive polarized neutron technique, can provide direct evidence for or against the model of the phase transition outlined above. Since the magnetic signal is much smaller than that observed for Ni₂MnGa, it is not possible to measure the magnetic structure factors with sufficient precision to determine a change in symmetry of the magnetization distribution. However, it is possible to determine the magnitude of the vanadium susceptibility on different sites in the transformed phase. In the high-temperature cubic A15 phase the vanadium atoms occupy 6e sites (space group $Pm\bar{3}n$) which, in the tetragonal phase (space group $P4_2/mmc$), split into two non-equivalent subsets 2e with site symmetry $\bar{4}2m$ and 4k with symmetry mm . The band Jahn–Teller model then predicts that, on cooling through the transition, the distributions of electrons in the sub-bands at the 2e and 4k sites should become different; consequently the local densities of states at the Fermi surface and hence the susceptibilities of the 2e and 4k sites should differ.

4. Experimental procedure

4.1. Material

The single crystal of V₃Si used in the experiments was grown from the melt using the Bridgman technique; it was cylindrical in shape with length 3 mm and diameter 2.4 mm. Magnetization

measurements undertaken with a SQUID magnetometer showed anomalies at 17 and 21.3 K consistent with the reported superconducting and martensitic phase transitions, respectively.

4.2. Unpolarized neutron measurements

Measurement of the integrated intensity of all reflections with $\sin(\theta)/\lambda < 1 \text{ \AA}^{-1}$ were made on the diffractometer D9 at the ILL Grenoble using a wavelength of 0.84 Å. The crystal was maintained in the tetragonal phase at 15 K using a two-stage Displex refrigerator mounted on the χ -circle of the Eulerian cradle. The resolution of D9 is not good enough to show the tetragonality of the structure, so the data were treated as though the symmetry were cubic. The intensities of cubically equivalent reflections were averaged together and a mean observed structure amplitude for each set of equivalents was calculated. The agreement between the equivalent reflections was good, leading to a merging R -factor of 1.8% for F^2 . The average structure was refined, allowing a small degree of extinction; the final agreement factor R calculated for the structure factors was 1.5 with a mosaic spread parameter of $0.97(12) \times 10^{-4} \text{ rad}^{-1}$.

4.3. Polarized neutron diffraction

The polarized neutron diffraction experiments were carried out at the ILL Grenoble using the D3b diffractometer, which receives an incident beam from the hot source. In order to favour one of the three possible tetragonal twins, the crystal was cooled through the martensitic phase transition in a magnetic field of 10 T. The transition is reported to take place by a combination of two shear distortions on {110} planes at 60 degrees to one another. Inelastic neutron scattering and ultrasonic measurements have shown that the corresponding {110} TA phonon modes soften near T_M . If a magnetic field is applied along a cube axis, the soft mode of lowest energy is in the plane perpendicular to it [18]. Therefore, cooling the crystal in a magnetic field parallel to [120], for which the modes of lowest energy are in the planes 101, $10\bar{1}$, 011 and $01\bar{1}$, should result in the tetragonal axis of the transformed crystal being parallel to [001]. The crystal was mounted with [120] approximately parallel to the axis of a 10 T split-pair superconducting magnet. This axis is also the axis of the diffractometer, which enabled measurements to be made of reflections hkl with $4 \geq h - 2k \geq 0$. The differences between the magnetic scattering in the hkl and lkh pairs of reflections contain information about the inequivalence of the magnetization of the e and k vanadium sites. In the experiment, eight such pairs and three triplets, hkl , klh , lkh , with $\sin(\theta)/\lambda < 0.5$ were measured in an applied field of 10 T. The magnetic susceptibility of V_3Si is $0.5 \times 10^{-3} \text{ cm}^3 \text{ mol}^{-1}$ so the moment aligned by 10 T is only $\approx 10^{-2} \mu_B/\text{cell}$. The differences from unity of the flipping ratios were of order 10^{-2} . To obtain reasonable precision, each reflection had to be measured for 4–6 hours. All accessible symmetrically equivalent reflections were measured in order to enable assessment of the internal consistency of the results.

5. Analysis of the data

The thermal and extinction parameters obtained from the unpolarized neutron data were used to calculate the magnetic structure factors from the flipping ratios measured using polarized neutrons. The calculation took into account incomplete polarization of the incident beam, the inclination of the scattering vector to the magnetic field direction and extinction. The results are given in table 2. Although the differences are not individually very significant, statistical

Table 2. The moduli of the magnetic structure factors measured for groups of reflections hkl which are equivalent with cubic symmetry, but distinct in the tetragonal phase. The values are given in μ_B per cell.

h	k	l	$ F_{hkl} $	$ F_{lkh} $	$ F_{lhk} $
1	0	1	0.0118(7)	0.0129(3)	
1	0	2	0.0131(7)	0.0127(8)	
1	1	2	0.0076(6)	0.0078(8)	
2	0	2	0.0055(8)	0.005(8)	
1	0	3	0.0046(10)	0.0062(15)	0.0047(14)
2	0	3	0.013(3)	0.017(4)	0.007(2)
2	1	3	0.0023(12)	0.0065(19)	0.0044(13)
3	0	3	0.0053(12)	0.0025(10)	
1	1	4	0.0030(13)	0.003(2)	
2	0	4	0.006(2)	0.005(2)	
2	1	4	0.006(3)	0.002(3)	0.006(2)
3	2	2	0.001(2)	0.001(2)	

analysis suggests that the probability of them all being due to random error is very small. Further analysis is therefore justified.

The magnetic structure factors of table 2 were fitted using a model in which the magnetization associated with vanadium sites has a distribution given by the V^{2+} spherical free-atom form factor. The only parameters of the model were the moments induced on the two sites. A least-squares fit gave moments of $(8.8 \pm 0.5) m \mu_B$ at the twofold e site and $(6.3 \pm 1.1) m \mu_B$ at the fourfold k site.

6. Discussion

Ideally, these results should be interpreted in terms of a full band-structure calculation, but for simplicity we shall discuss the qualitative consequences of the Labbé–Friedel model. Figure 2 shows schematically the arrangement of the $d_{x^2-y^2,xy}$ bands at E_F postulated by Labbé and Friedel in (a) the cubic and (b) the tetragonal phase. In this discussion we define [001] to

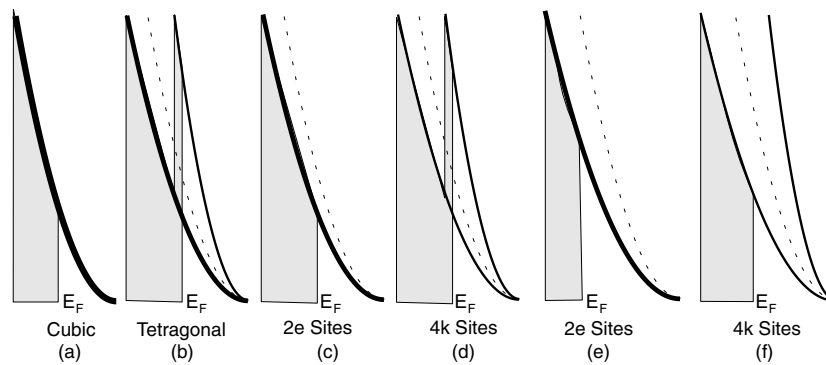


Figure 2. A schematic representation of density of states in the partly filled $d_{x^2-y^2,xy}$ bands in V₃Si (after [12]). The filled areas represent occupied states; degenerate bands are indicated by thick lines. The fine dashed lines in (b) to (f) indicate the positions of the bands with no tetragonal distortion

be parallel to the fourfold axis in the tetragonal phase. The quantum z -axis for each V site is chosen parallel to the axis of the chain to which it belongs. In the tetragonal phase the $d_{x^2-y^2,xy}$ orbitals of V atoms whose quantum z -axis is parallel to [001], the unique axis, remain degenerate. Those on atoms with the quantum z -axis parallel to [100] or [010] split. With $c/a > 1$ as in V_3Si , those for which the x - or y -axis is parallel to [100] or [010] are wider than those for which one or other is parallel to [001]. The schematic DOS in these bands for the crystal as a whole is as in figure 2(b) and for the 2e and 4k sites separately as in figures 2(c) and 2(d). As pointed out by Labbé and Friedel, there are two different possibilities: either the distortion is small, with the result that the Fermi surface remains above the bottom of both bands, or it may lie below the bottom of the narrower band. In the former case the DOS in the narrow band will always be higher than that in the wider one. At the 2e sites there are two degenerate wide bands of this type and at the 4k sites a wide and a narrow one as shown in figures 2(c) and 2(d). Therefore, as long as the Fermi level is above the bottom of the narrow band, the susceptibility of the 4k sites should be higher than that of the 2e ones. Labbé and Friedel show that in this case, in which the Fermi level intersects both bands, the decrease in energy is only quadratic in the distortion. On the other hand, if the distortion and band occupancy are such that the bottom of the narrow band lies above E_F , then the situation is quite different (figures 2(e) and 2(f)). The change in energy becomes linear in the distortion and the DOS at the Fermi surface is entirely due to electrons in the wide bands. Since there are two wide bands at the 2e sites and only one at the 4k sites, the susceptibility of the 2e site should be the larger, as found in the experiment.

7. Conclusions

The difference between the local susceptibilities at the two independent V sites in the tetragonal non-superconducting phase of V_3Si has been determined using polarized neutron diffraction. This difference was demonstrated by comparing the polarization dependence, induced by a high magnetic field, in the intensities of reflections which become inequivalent in the cubic-to-tetragonal phase transition. The difference in site susceptibilities which was observed lends support to models of the phase transition based on a band Jahn–Teller effect. These results demonstrate the ability of polarized neutrons to access the local (site-specific) magnetic response from which it is possible to infer details of the electronic structure, thus contributing to a field which is not traditionally associated with neutron scattering.

Acknowledgments

The authors would like to thank W Weber for helpful discussions and B Dennis for making the magnetization measurements.

References

- [1] Testardi L R 1975 *Rev. Mod. Phys.* **47** 637
- [2] Batterman B W and Barrett C S 1964 *Phys. Rev. Lett.* **13** 390
- [3] Hirota K, Rebelsky L and Shirane G 1995 *Phys. Rev. B* **51** 11 325
- [4] Shirane G and Axe J D 1971 *Phys. Rev. Lett.* **27** 1803
- [5] Fujii Y, Hastings J B, Kaplan M, Shirane G, Inada Y and Kitamura N 1981 *Phys. Rev. B* **1** 364
- [6] Fawcett E 1971 *Phys. Rev. Lett.* **26** 829
- [7] Maita J P and Bucher E 1972 *Phys. Rev. Lett.* **29** 931
- [8] Krumhansl J A and Goodings R J 1989 *Phys. Rev. B* **39** 3047
- [9] Kunzeler J E, Maita J P, Levinstein H J and Ryder E J 1966 *Phys. Rev.* **143** 390

-
- [10] Vieland L J and Wicklund A W 1969 *Solid State Commun.* **7** 931
 - [11] Gossard A C 1966 *Phys. Rev.* **149** 246
 - [12] Labbé J and Friedel J 1966 *J. Physique* **27** 153
 - [13] Weger M 1964 *Rev. Mod. Phys.* **36** 175
 - [14] Weber W and Mattheiss L F 1982 *Phys. Rev. B* **25** 2270
 - [15] Mattheiss L F and Weber W 1982 *Phys. Rev. B* **25** 2248
 - [16] Toyota N, Kobayashi T, Kataoka M, Watanabe H F J, Fukase T, Muto Y and Takei F 1988 *J. Phys. Soc. Japan* **57** 3089
 - [17] Brown P J, Bargawi A Y, Crangle J, Neumann K-U and Ziebeck K R A 1999 *J. Phys.: Condens. Matter* **11** 4715
 - [18] Dieterich W and Fulde P 1971 *Z. Phys.* **248** 154